

CAMELS-FR dataset: A large-sample hydroclimatic dataset for France to explore hydrological diversity and support model benchmarking

Olivier Delaigue¹, Guilherme Mendoza Guimarães¹, Pierre Brigode^{1,2,3}, Benoît Génot^{1,4}, Charles Perrin¹, Jean-Michel Soubeyroux⁵, Bruno Janet⁶, Nans Addor^{7,8}, and Vazken Andréassian¹

¹Université Paris-Saclay, INRAE, HYCAR, Antony, France

²Université Côte d’Azur, CNRS, OCA, IRD, Géoazur, Sophia-Antipolis, France

³Université de Rennes, CNRS, Géosciences Rennes, Rennes, France

⁴Now at U.R.B.S., Saint-Étienne, France

⁵Météo-France, DCSC, Toulouse, France

⁶Service central d’hydrométéorologie et d’appui à la prévision des inondations (MTES/DGPR/SCHAPI), Toulouse, France

⁷Fathom, Bristol, UK

⁸Geography, University of Exeter, Exeter, UK

Correspondence: Olivier Delaigue (olivier.delaigue@inrae.fr)

Abstract. Over the last decade, large-sample approaches, i.e. based on large catchment sets, have become increasingly popular in hydrological studies. Efforts were made to assemble and disseminate national catchment datasets. This article aims to add a stone to the construction of a large international database of catchments by proposing the CAMELS-FR dataset, a contribution to the CAMELS initiative (Catchment attributes and meteorology for large-sample studies). The first version presented here gathers hydroclimatic data and physical attributes for a set of 654 catchments in France. These catchments cover a wide spectrum of hydroclimatic conditions (from oceanic to continental, mountainous or Mediterranean conditions), and are considered to have limited human influence. Data include time series of daily streamflow (with at least 30 years over the 1970-2021 period; also aggregated to monthly and yearly time steps) and of eleven catchment-scale daily climate variables (including precipitation, potential evaporation, and air temperature), as well as a total of 255 catchments attributes organised in ten classes (e.g. geology, soil, land cover, etc.). River flow time series were quality-checked. Along with the database itself, two graphical tools are proposed, namely dynamic graphs to visualize time series and graphical fact sheets to summarize the main catchments characteristics. Care was taken to provide as many metadata as possible to help users interpret their results based on this dataset. We intend to update the database regularly to include new available data and account for end-users’ feedbacks.

1 Introduction

In the early days of hydrological modelling, access to data, followed by computing resources, was a major limiting factor of progress, and many of the scientific articles of that time reported results obtained on a single catchment (and sometimes using only a few flood events). The precursors of modern hydrological models were conscious that this was a major shortcoming. Linsley for example did recommend (1982, p. 15) that "because almost any model with sufficient free parameters can yield

good results when applied to a short sample from a single catchment, effective testing requires that models be tried on many
20 catchments of widely differing characteristics, and that each trial cover a period of many years." Roughly 20 years later, under
the tireless leadership of John Schaake, the so-called *MOPEX* dataset started to be used worldwide (Schaake et al., 2006),
blowing a refreshing wind on the hard-drives of data-thirsty modellers. Ten years later, the paper published by Gupta et al.
(2014) presented an already impressive list of 94 "large-sample" studies focusing on rainfall-runoff modelling, which had used
a dataset of more than 30 catchments. Today, the number of such studies would probably be multiplied by 10, and it has
25 become almost impossible to keep track of all of them. Obviously, computing time difficulties and data sharing possibilities
have completely changed.

In France, there has been a long tradition of working with large datasets, following the recommendations of two French
leading hydrologists of the 20th century: Maurice Pardé and Marcel Roche. Later however, large datasets were sometimes
mocked as "hydro-bulimia" (Andréassian et al., 2009), and during a certain time, the academic world favoured the production
30 of individual basin monographs rather than modelling studies involving large datasets. Over the last decade, progresses were
made towards automatizing the production (and the updating) of large catchment datasets. In collaboration with the main data
producers of hydrometric and meteorological data, we worked to produce the reference hydrological dataset that we present
in this paper. For the selection of this dataset, we used what we considered to be "high" quality standards, and because we
do acknowledge that there is a part of subjectivity in this, let us paraphrase Ghislain de Marsily in his comment on model
35 validation and state that we strove to do "our level best" (de Marsily et al., 1992), using a variety of automatic data verification
procedures, which were complemented by manual checks (including a time-consuming —but clearly necessary— visual data
inspection).

With this work, we wish to contribute to the general effort to provide large hydroclimatic datasets as it was done in the United
States of America (Newman et al., 2015; Addor et al., 2017), Canada (Arsenault et al., 2016), Chile (Alvarez-Garreton et al.,
40 2018), Great Britain (Coxon et al., 2020), Brazil (Chagas et al., 2020; Almagro et al., 2021), Australia (Fowler et al., 2021),
Central Europe (Klingler et al., 2021), Africa (Tramblay et al., 2021), Denmark (Koch, 2021; Liu et al., 2024), Switzerland
(Höge et al., 2023), Saxony (Hauffe et al., 2023), Germany (Loritz et al., 2024), and next to the many others that will follow.
As a national dataset, CAMELS-FR should also be seen as complementary to other datasets built at larger scales that include
France, e.g. the EStreams dataset at European scale (do Nascimento et al., 2024a, b). CAMELS-FR differs from such datasets
45 in the criteria used in the catchment selection process, the data analysis methods and the choices in data sources that may be
available at national but not larger scales.

Before moving to the presentation of the dataset, let us warn the reader that for reasons of scientific ethics, we refused
to exclude hydrological "outliers" (i.e. catchments that exhibit unusual hydrological behavior: e.g. karstic catchments, or
groundwater-dominated catchments fed by the chalk aquifer of the Parisian Basin, and having very high baseflow indices)
50 from the CAMELS-FR dataset. We did so because we believe that the outliers are part of the "natural hydrological diver-
sity" (Andréassian et al., 2010), and also because from a scientific point of view, even good-looking catchments can turn into
a "modeller's nightmare" (Refsgaard and Hansen, 2010). This is why we did keep for example the karstic catchments which
have been excluded from other datasets. Note that other catchment sets at the national scale already exist in France for more



Figure 1. Map of the main geographical features of France: mountain ranges (text with white outline), regions (text without outline), and main basins (pink: Seine; yellow: Loire; orange: Garonne; purple: Rhône) (river network: Lehner and Grill, 2013; DTM: Lehner et al., 2008; shoreline & political boundaries: Wessel and Smith, 1996; NOAA, 2017).

specific purposes, for example the Reference Low Flow Network to study the long-term evolution of low flows (see Giuntoli et al., 2013; Hodgkins et al., 2024), and elsewhere (see a review of large-sample studies in Gupta et al., 2014).

2 French physical and hydroclimatic context

2.1 Physical characteristics

Metropolitan France (mainland France and Corsica; see Fig. 1), covers an area of 550,000 km² (expanding 1,000 km from north to south, and east to west), including Corsica, the fourth largest Mediterranean island (8,700 km²). It is mainly bounded by coastlines (with the North Sea, the English Channel, the Atlantic Ocean and the Mediterranean Sea) and shares terrestrial borders with eight neighboring countries (Belgium, Luxembourg, Germany, Switzerland, Italy, Monaco, Spain, Andorra). Metropolitan France offers a wide variety of natural landscapes inherited from several geological phases, giving rise to ancient (e.g. Armorican Massif, Massif des Vosges, and Massif Central) and younger mountain ranges such as the Jura, Alps and Pyrenees (see Fig. 2a). The average altitude is 344 m, and the elevation reaches a maximum of 4,806 m at Mont Blanc (in the Alps). These mountain ranges form the boundaries of several sedimentary basins, including the Aquitaine Basin in the southwest and the Paris Basin to the north.

The French geological diversity is illustrated with the wide range of colors found on the lithological map of France (see Fig. 2c). We give here a short description of the (complex) geology of France, focusing on its implications for understanding the hydrogeology of French catchments. A more detailed account is provided by Pelletier (2021):

- 70 – A quarter of France is covered by basement rocks that are metamorphic or igneous in origin. Basement formations host small local aquifers, but no large-scale aquifers. The two main areas are the Armorican Massif in the northwest, almost exclusively composed of ancient formations, and the Massif Central in the center of the country (a more complex area where Hercynian basement, sedimentary formations and recent volcanic formations coexist). Basement rocks also outcrop in smaller massifs of lesser extent (e.g. the Massif du Morvan in the upper Yonne basin, the Massif des Albères at
75 the border of France and Spain in Catalogne, the Massif ardennais around the Meuse River at the border with Belgium, the Massif de la Serre in the Jura Mountains near the Swiss border and the Massif des Maures on the Mediterranean coast near Saint-Tropez). Note that the Massif des Vosges is divided between basement formations to the south and sedimentary formations to the north;
- Intensely folded areas are hydrogeologically very complex, because in these regions, aquifers, if they exist, are of limited
80 spatial extent and therefore difficult to identify for mapping on a regional or national scale. These areas correspond to the most recent massifs: the central and inner part of the Alpine arc, the Pyrenees and the Languedoc massifs;
- The rest of the territory is occupied by two main types of formations: sedimentary formations, and alluvial plains. The sedimentary formations form two major basins: the Paris Basin, which covers a third of Metropolitan France, and the Aquitaine basin in the southwest. Formed by sedimentary deposits left by marine intrusions, they appear as a succession
85 of geological layers with diverse aquifer properties, whose outcrop areas form rings, known as the "pile d'assiettes" (plate stack) in the Paris Basin;
- Alluvial plains and the accompanying aquifers are formed by the scouring and degradation by rivers of various materials, which are then deposited along the river bed. In mainland France, they are generally of limited geographical extent, unlike in other parts of the world. Two alluvial aquifers, however, are of greater importance: they are located in the upper Rhine
90 plain in Alsace, and in Bresse (around the Saône River, north of Lyon).
- the variability of surface aquifer properties is clearly apparent when one looks at the density of the observed river network in Fig. 2c, where for example the large areas underlain by chalk formation in the Paris Basin stand out with their much lower drainage density, while the Champagne Humide region, characterized by clayey and loamy soils, has a much denser river network. The Beauce region, underlain by the Beauce limestones aquifer complex, is clearly visible as a
95 white spot southwest of Paris at the border of the Seine and the Loire basins.

In 2015, farmland covered around 51 % of Metropolitan France, compared with around 40 % for soils not directly subject to anthropogenic pressures (woodlands, wetlands and water surfaces) and around 9 % for artificialized soils (see Fig. 2d).

2.2 Hydro-climatic characteristics

According to the Köppen-Geiger climate classification (see e.g. Peel et al., 2007; and [Strohmenger et al., 2023](#) [Strohmenger et al., 2024](#) for a recent analysis on France), more than 90 % of the French territory belongs to the *Cfb* class (i.e. temperate without dry season and with warm summers), with Corsica and the Mediterranean shore belonging to the *Csa* or *Csb* classes (temperate with dry and respectively hot or warm summers). The mountain ranges belong to class *Dfb* (continental without dry season and warm summers), *Dfc* (continental without dry season and cold summers), and the high-elevation summits belong to the *ET* class (polar climate). Average annual precipitation ranges from 500 mm yr⁻¹ for the driest regions (e.g. Mediterranean coasts) to more than 2,000 mm yr⁻¹ in mountainous regions (see Fig. 2e and 2f). While precipitation usually varies in a progressive manner over much of the country, a few mountain ranges are characterized by strong differences: one can mention for example the Cévennes range in the south, where average rainfall reaches 2,000 mm yr⁻¹, located not far from the Crau lowlands, where average rainfall is less than 500 mm yr⁻¹. A similar situation exists near the Rhine valley in Alsace, where average rainfall in the Massif des Vosges reaches 2,000 mm yr⁻¹ while it is less than 500 mm yr⁻¹ in the Colmar plain. As far as temperature is concerned, it is probably enough to mention the mild winter temperatures on the ocean coast and the Mediterranean sea, the lowest temperatures being reached on the high mountain ranges where a few glaciers still exist despite the global warming trend.

The Metropolitan France's hydrographic network (Fig. 2b) is mainly organized around four major rivers (the Loire, Seine, Garonne and Rhône), whose catchments cover more than 60 % of mainland France. The Rhône and the Garonne catchments are transboundary, with their sources in Switzerland and Spain respectively. Other transboundary rivers are found in France such as the Meuse (crossing France, Belgium and the Netherlands), the Rhine (crossing Switzerland, Liechtenstein, Austria, Germany, France and the Netherlands), and the Roya (crossing France and Italy), among others (e.g. the Sarre, the Oise, etc.). The French rivers are characterized by different hydrological regimes, with rain-dominated catchments, both rain- and snow-dominated catchments, snow-dominated catchments, Mediterranean catchments, and groundwater-dominated catchments. The most upstream parts of a few mountainous catchments are still influenced by glaciers. In Metropolitan France, glaciers are located in the Alps and in the Pyrenees. Most of them cover rather small areas, especially when related to the area of catchments. The two main glaciers are the Argentière glacier and the Mer de Glace, in the Mont Blanc massif. Due to climate change, Vincent et al. (2019) showed that these two glaciers lost 34 and 45 m of water-equivalent depth, respectively, since the beginning of 20th century, representing 25 and 32 % of their thickness, respectively. Some other glaciers are located in the Ecrins and Vanoise massifs.

Most of France's catchments are impacted by human activities through the presence of large dams (for water supply, hydropower or flood and low-flow management), river abstraction and groundwater pumping for agricultural, industrial, and drinking water use, therefore we aimed to exclude the most influenced catchments. The location of the main French reservoirs are shown in Fig. 2a. Note that a large number of small artificial water bodies exists in France, for various uses (recreation, irrigation, boating, fishing, etc.), but often with more limited information available.

2.3 Main data producers

The French hydrosystems have been monitored for several decades through various observational networks, maintained by different organizations. These mainly include national agencies such as Météo-France for climatic data, the French geological survey (*Bureau de recherches géologiques et minières*, BRGM) for geological and hydrogeological information, the National
135 Institute of Geographic and Forest Information (*Institut national de l'information géographique et forestière*, IGN) for geographic and forest information, and different State services and independent producers (e.g. EDF, CNR, universities, etc.) for hydrological data. These streamflow data are made available by the Central service for hydrometeorology and inundation forecasting (*Service central d'hydrométéorologie et d'appui à la prévision des inondations*, SCHAPI).

3 Catchment boundaries

140 The first step to build the `CAMELS-FR` dataset was to delineate the contours of the catchments boundaries, which were then used to calculate hydroclimatic time series at this scale.

3.1 Making a flow direction grid to delineate catchment boundaries at national scale

Hydrological analysis and modelling require to associate climatic forcing averaged at the catchment scale with the streamflow measurements recorded at the outlet of a catchment. It was therefore necessary to identify the geographic extent of all French
145 catchments.

To do so, we used a flow direction grid, i.e. a matrix summarizing the topological relationships for Metropolitan France. This grid is derived from a topographic analysis of two digital terrain models (DTMs). For continental Metropolitan France, we used the DTM from the Shuttle Radar Topography Mission (SRTM) project with resolution of $100 \times 100 \text{ m}^2$ (Rabus et al., 2003; Farr et al., 2007), and for Corsica, we used the BD ALTI v1.0 from the IGN (2001) with resolution of $25 \times 25 \text{ m}^2$.

150 Because no DTM is error-free, we used an "observed" river network to force the geometry of the theoretical river network to be closer to reality. To constrain the flow directions via the stream-burning method, we used the CARTHAGE river network (French water agencies, 2017b) with removed channels. This method consists in initially burning the vector network in the DTM by artificially lowering the altitude of the pixels belonging to the network. For more details about the method, see Bourgin et al. (2010).

155 3.2 Geographic repositioning of hydrometric stations on the flow direction grid

When the metadata linked to the gauging stations are well filled in, the geographical coordinates (latitude, longitude and altitude) and the area of the upstream catchment of the station are available. However, this information is not always consistent with the flow direction grid that we made. Sometimes the resolution of DTM is not sufficient, sometimes the gauging station's coordinates are erroneous or not sufficiently precise. Repositioning geographically the hydrometric stations on the calculated

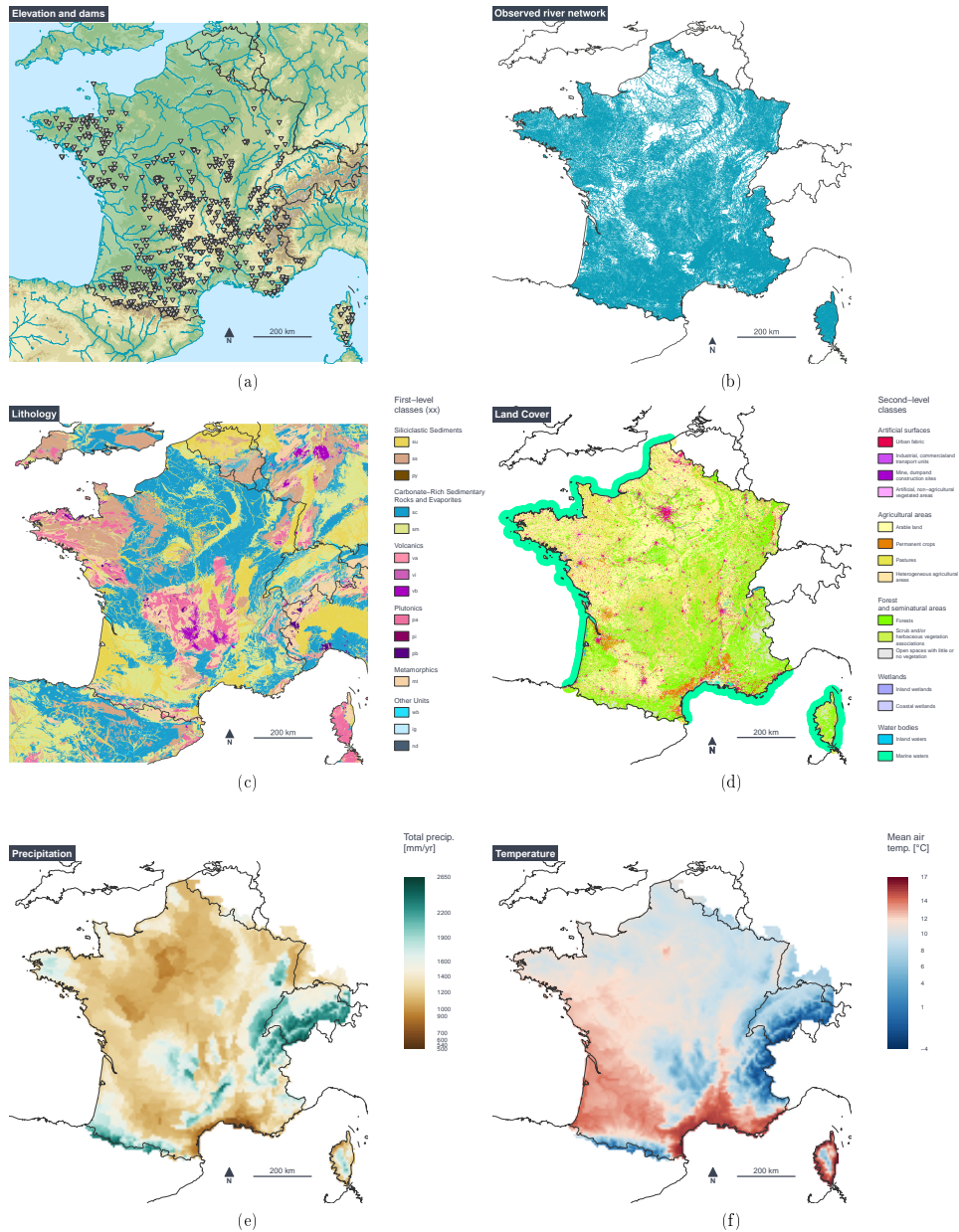


Figure 2. Maps describing Metropolitan France territory. (a) Elevation, main rivers and main dam locations (triangles) (river network: Lehner and Grill, 2013; DTM: Lehner et al., 2008; shoreline & political boundaries: Wessel and Smith, 1996; NOAA, 2017); (b) Observed river network (CARTHAGE: French water agencies, 2017b); (c) Lithology (GLiM v2.0: Hartmann and Moosdorf, 2012; *su*: unconsolidated sediment, *ss*: siliclastic sedimentary rocks, *py*: pyroclastics, *sc*: carbonate sedimentary rocks, *sm*: mixed sedimentary rocks, *va*: acid volcanics, *vi*: intermediate volcanics, *vb*: basic volcanics, *pa*: acid plutonics, *pi*: intermediate plutonics, *pb*: basic plutonics, *mt*: metamorphics, *wb*: water bodies, *ig*: ice and glaciers, *nd*: non-defined); (d) Land cover (CLC: French Ministry of the Environment, 1990); (e) Mean annual total precipitation over the 1991-2020 period (SAFRAN: Quintana-Segui et al., 2008; Vidal et al., 2010); (f) Mean air temperature over the 1991-2020 period (SAFRAN).

160 flow direction grid is therefore often necessary. Each hydrometric station must be linked with the "river" pixel of the flow direction grid. Only then can the contour and area of the catchment be delineated.

For the gauging stations that are not positioned in a "river" pixel, we searched in the twenty-four surrounding pixels (i.e. radius of 200 m for the continental Metropolitan France) the theoretical position of the gauging station by iteratively calculating the catchment area located upstream of each surrounding pixel. The objective is then to minimize the difference between the
165 area indicated by the data producer (if available) and the area calculated on the flow direction grid. This method allows to automatically place a large part of the hydrometric stations on the flow direction grid.

However, errors still exist ~~on~~in some stations. Therefore, all outlets were checked manually using a graphical user interface (GUI) we developed for this specific goal (Génot and Delaigue, 2018). This GUI (see screenshot on Fig. 3; not made available with the dataset) provides means to analyze the geographical location of the hydrometric station by visualizing maps (e.g.
170 maps, or aerial photos), and the comparison between the observed and the theoretical river networks, but also by facilitating the comparison of catchment areas.

4 Selection of the catchment set

The second step to build the CAMELS-FR dataset was to select the catchments based on the following criteria: (i) hydro-metric time series availability (Sect. 4.1), (ii) limited artificial reservoirs influences (Sect. 4.2), (iii) consistency in catchment
175 areas (Sect. 4.3), (iv) ~~streamflow quality inspection~~sufficient streamflow quality (Sect. 4.4).

The application of the different criteria and analyses described in the following subsections resulted in the selection of 654 catchments, constituting the CAMELS-FR dataset v1.

4.1 Selection on hydrometric time series availability

We excluded catchments with less than 30 years of complete data over the 1970-2021 period. This record length was arbitrarily
180 chosen because it allows robust statistical analyses. A year was considered complete when it had less than 20 % of missing data. This criteria was responsible for removing approximately 70 % of all stations available in France.

4.2 Artificial reservoirs influences

Our objective was to only select catchments displaying a level of human disturbance as low as possible. Here, we only consider influences due to artificial reservoirs. Therefore, the MADAM dataset v1.0 (Delaigue et al., 2024b) was used to estimate these
185 influences. To build this dataset, two sources of information were used, namely the work of Payan (2007) & Payan et al. (2008), and the GEOBS datasets (OFB and partners, 2023), in order to provide locations and volumes of dams in Metropolitan France (mainland and Corsica). Each time, we calculated a theoretical level of influence by estimating the equivalent water depth of the total water storage capacity of all dams on the catchment (sum of capacities divided by catchment area).

We cross-checked the two sources of information. The positions of the dams were manually checked. When the storage
190 capacity was inconsistent among the datasets, we validated the dam volume using the website of the French Committee for

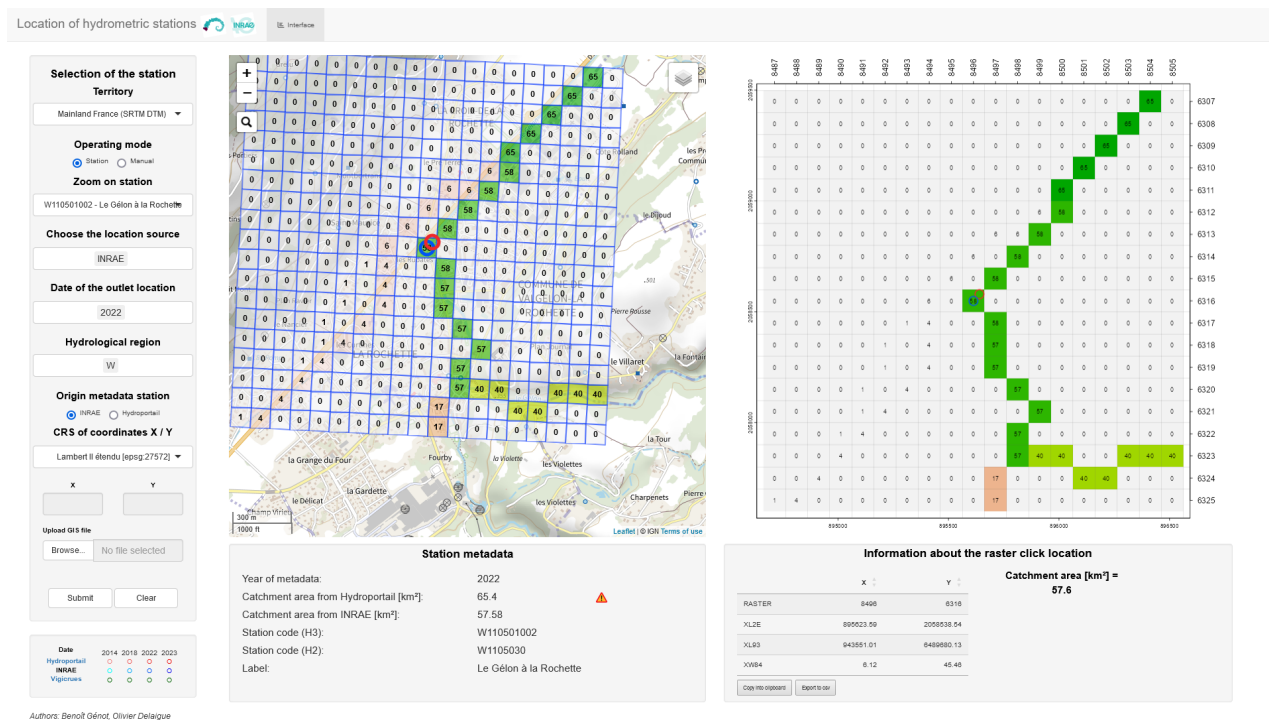


Figure 3. Screenshot of the graphical user interface helping to relocate hydrometric stations on the theoretical river network (Génot and Delaigue, 2018). The left panel is for option selection where we can select the territory (mainland France or Corsica), a specific station by providing its code or by directly inputting the coordinates, and the metadata year. The middle panel shows the zoomed location of the station on a map layer ("Plan IGN" v2 map layer, IGN, 2020), a superposition of the raster layer with contributing area grid to aid identifying the correct location of the hydrometric stations. The producer's gauging station is in red circle, and INRAE's location snapped on the theoretical river network is in blue circle. The metadata for the searched gauging station are displayed below this map. On the right panel the contributing area grid and the hydrometric station locations are displayed a new time allowing to click on the map, and to extract the raster information such as pixel location and its corresponding catchment area.

Dams and Reservoirs (*Comité français des barrages et réservoirs*, CFBR, 2023), by collecting information from various technical documents of the operators freely available on the Internet, or by directly contacting the operators.

Only the catchments with an equivalent water depth of storage capacity lower than 10 mm were selected, thus removing catchments considered highly influenced from our selection. This threshold comes from experience on past studies on this issue (e.g. Payan et al., 2008), but remains arbitrary. The actual level of influence may depend on the local context (location of the dam(s) within the catchment, management objectives of the dam(s), etc.). But we preferred to stick to a single threshold value to have an homogeneous selection criterion.

Note that other types of influence may significantly modify natural streamflow in the selected catchments, typically water withdrawals for various uses or inter-basin water transfers. However since this information could not be accessed and processed

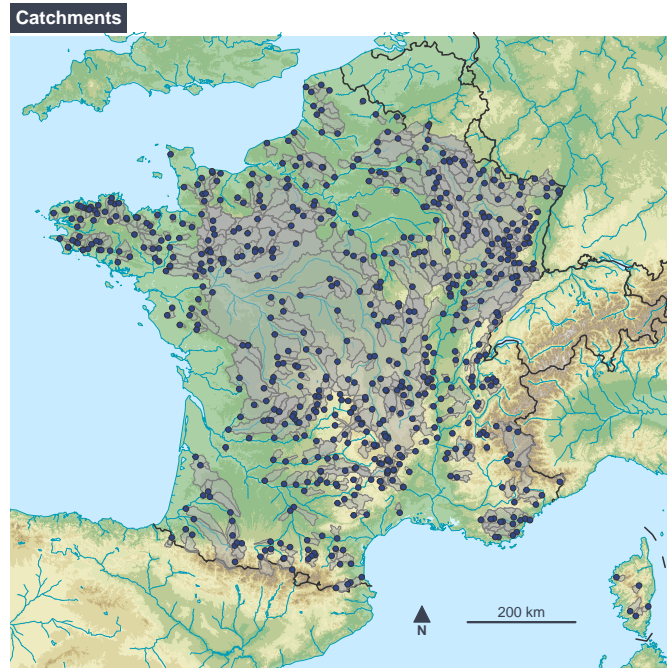


Figure 4. Location map of the 654 catchments and their outlets of the CAMELS-FR dataset v1 (river network: Lehner and Grill, 2013; DTM: Lehner et al., 2008; shoreline & political boundaries: Wessel and Smith, 1996; NOAA, 2017).

200 easily, it was not considered here as selection criterion. Thus, the CAMELS-FR catchment set should not be considered as strictly non-influenced catchments. For this reason, we also include in the catchment attributes descriptors giving the qualitative estimation of the local and general impact of human influences as provided by the data producers.

4.3 Consistency in catchment areas

The repositioning of the catchment outlets (reported by the data producers, alongside the catchment area) on the flow direction
 205 raster was manually checked. We wished to have similar catchment areas between the automatically computed procedure using the flow direction raster and the information provided by the data producers. The catchments whose areas differ by more than 10 % were discarded from the selection. Further investigation would be needed to clarify the reasons for these differences, which may lead to have additional catchments in the CAMELS-FR dataset in the coming years. For example, there may exist two types of catchment area (topographic and hydrogeologic) for karstic catchments in the metadata provided by the
 210 producers.

4.4 Streamflow quality inspection

Finally, a visual analysis of streamflow time series was performed in order to identify obvious errors in the streamflow series, such as flow interpolation, sudden drops and noises not referenced as so. The time series were evaluated by four observers. If

at least two observers considered a time series to be incorrect, it was removed from the dataset. If only one observer deemed a
215 time series incorrect, it underwent group re-evaluation to get a consensus on the data quality. Catchments with such errors have
been discarded from the dataset, pending for data correction from the data producers. This qualitative analysis of streamflow
series may lead the addition (or removal) of catchments in the CAMELS-FR dataset in the coming years. The difficulty
of detecting non-natural records in streamflow time series has been recently illustrated and discussed by Strohmenger et al.
(2023) on a large set of French catchments.

220 5 Hydroclimatic time series

5.1 Climatic time series

The SAFRAN atmospheric reanalysis (Quintana-Segui et al., 2008; Vidal et al., 2010) was used as source of daily climatic
time series, aggregated at catchment scale. SAFRAN is a mesoscale analysis system of near-surface atmospheric variables
from the SAFRAN-ISBA-MODCOU hydrometeorological model chain (SIM2; Le Moigne et al., 2020). The SAFRAN data
225 are provided annually by Météo-France at the daily time step from 1958 to present, and there is no missing data. The reanalysis
methodology is regularly updated and data is updated retroactively (since 1958). SAFRAN uses surface observations combined
with data from meteorological models, in particular the ERA reanalysis of the European Centre for Medium-Range Weather
Forecasts (ECMWF). Climate variables are analyzed by 300 m altitudinal steps. They are then interpolated on a regular grid
with resolution of $8 \times 8 \text{ km}^2$ (note that catchment rainfall is interpolated from ground measurements). The climatic data cover
230 the whole metropolitan territory (mainland France and Corsica), as well as areas at the borders to correspond to the catchments
of rivers flowing into France, with a total of 9,892 pixels. An evaluation of the SAFRAN reanalysis is provided in Vidal et al.
(2010).

The SAFRAN variables used in the CAMELS-FR dataset are: solid precipitation, liquid precipitation, air temperatures
(minimum and maximum), wind speed, specific air humidity, atmospheric and visible radiations. In addition, these climatic
235 data feed a soil-vegetation-atmosphere (SVAT) model called ISBA (Le Moigne et al., 2020) to produce surface variables,
such as snow water equivalent and a soil wetness index. Table 1 lists these variables and if they represent daily means or daily
accumulations. Note that the aggregation time window may differ between the variables considered, which may have an impact
on modelling results.

Using these variables, we calculated (i) three time series of potential evaporation estimates using three commonly-used
240 formulas: Penman (Penman, 1948), Penman-Monteith (Monteith, 1965) and Oudin (Oudin et al., 2005), and (ii) a soil moisture
index as computed by the GR4J rainfall-runoff model (Perrin et al., 2003, computed with a reservoir of 275 mm). Note that our
versions of Penman and Penman-Monteith formulas use a snow-dependent albedo.

The catchment-scale climatic time series are obtained by spatial aggregation of the SAFRAN pixels intersecting the catch-
ment contours. The SAFRAN variables are weighted-averaged using the pixel percentage within the catchment contour.

Table 1. List of daily SIM2 variables used in the CAMELS-FR dataset, and their aggregation methods at the daily time step.

SIM2 product	Variable	Unit	Aggreg. methods	Aggreg. time window [UTC]
SAFRAN	Solid precipitation	mm d ⁻¹	Accumulation	06 h–06 h
SAFRAN	Liquid precipitation	mm d ⁻¹	Accumulation	06 h–06 h
SAFRAN	Air temperature	°C	Mean	00 h–24 h
SAFRAN	Daily minimum air temperature	°C	-	00 h–24 h
SAFRAN	Daily maximum air temperature	°C	-	00 h–24 h
SAFRAN	Wind speed	m s ⁻¹	Mean	00 h–24 h
SAFRAN	Specific air humidity	g kg ⁻¹	Mean	00 h–24 h
SAFRAN	Atmospheric radiation	J cm ⁻² d ⁻¹	Accumulation	00 h–24 h
SAFRAN	Visible radiation	J cm ⁻² d ⁻¹	Accumulation	00 h–24 h
ISBA	Snow water equivalent	mm d ⁻¹	Accumulation	06 h–06 h
ISBA	Soil wetness index	–	Mean	06 h–06 h

245 **5.2 Hydrometric time series**

The SCHAPI released in January 2022 the Hydroportail application for accessing hydrometric data at the national scale. Hydroportail classifies the hydrometric entities into three levels: hydrometric site, hydrometric station and hydrometric sensor. The hydrometric site refers to a portion of a watercourse on which flows are considered homogeneous. Several hydrometric (gauging) stations can be associated with a single site. A hydrometric station may include several sensors. The main benefit
250 of dividing the hydrometric entities into these levels is to give the producers the possibility to set a calendar (i.e. periods of validity of each station and sensor) at the site level and unify the corresponding streamflow data to produce a consolidated time series with a better qualification procedure.

The CAMELS-FR dataset daily streamflow time series were retrieved from the Hydroportail website using the hydroportail R-package (Delaigue, 2022). Streamflow data were retrieved at the station level to get all the data even for sites
255 where calendar information is missing or incomplete. For stations with sub-daily streamflow data, mean daily streamflows are calculated using a trapezoidal method, thus assuming a linear variation in streamflow between successive instantaneous streamflows. This was done directly by the data producer or by the Hydroportail procedure.

Streamflow data are available in the CAMELS-FR dataset in ls⁻¹ and were also converted in water depth (in mm d⁻¹) using the catchment area derived from the DTM (and not producer’s area). As climatic data, the streamflow time series are
260 provided at the daily, monthly and yearly time steps.

5.3 Rules for time series aggregation

The time series are provided at the daily, monthly and yearly time steps. For the calculation of monthly time series, a month was considered missing if it had more than 3 days of missing data. The time series at yearly time step are provided using

Table 2. Number of catchment attributes in each class for the CAMELS-FR dataset v1. [\(the "Other" class is related to data access information\).](#)

Class	Nb.
Location & Topography	91
Climatic indices	51
Hydrometry	18
Hydrological signatures	24
Hydrogeology	11
Geology	17
Soil	25
Land cover	10
Intervention degree	7
Other	1

hydrological year (considered to start on 1 October) as basis of aggregation. Therefore the hydrological year of 1970 (first year
265 of the dataset), which starts on 1 October 1969, and is deemed incomplete because of the three first missing months. Moreover,
these yearly data are computed based on the above-mentioned monthly times series. If one month is missing, the whole year is
considered missing.

6 Catchment attributes

The CAMELS-FR dataset v1 contains 255 attributes, organized in 10 classes (see Tab. 2), described in the following sub-
270 sections. A spreadsheet listing each catchment attribute is included in the CAMELS-FR dataset.

6.1 Location

Most of the location attributes are information given by the data producer and extracted from Hydroportail. Such attributes
include the station codes, names, location, type of station, etc. The data producer gives, for most catchments, an estimate of
catchment area. Note that for some catchments this area is significantly different from the one derived from the DTM analysis
275 (see Sect. 4.3). Other catchment attributes were computed for the CAMELS-FR dataset. They include station coordinates
(after repositioning on the DTM-derived river network), catchment area (derived from the DTM), and information on the station
nestedness (indicating whether the catchment is nested, the number of stations downstream, etc.).

6.2 Topography

Two DTMs (NASA & NGA DTM from SRTM for catchments located on the continent and the BD ALTI v1.0 (IGN) for
280 catchments in Corsica) were used to estimate various attributes describing catchment topography, drainage density, and mor-

phometry. Among the topography attributes are the mean and the percentiles distribution for elevation, slope, distance to catchment outlet and topographic index. The methodology used to calculate the topographic index follows Ducharne (2009), which reformulates the index used in TOPMODEL (Beven and Kirby, 1979) to become a dimensionless index. The percentage of catchment slope classes (flat, gentle, moderate, strong, steep, and very steep) and orientation, and the classical drainage density which is measured as the ratio of total length of stream channels to catchment area (Horton, 1932) are also provided. Among the morphometry attributes, several catchment shapes indicators are provided. These include three variants of basin form factor (Horton, 1932; Zăvoianu, 1978, cited by Zăvoianu, 1985, p. 109; Subramanya, 2013, p. 172), the compactness coefficient (Fitzpatrick, 2017), the circularity ratio proposed by Miller (1953, cited by Zăvoianu, 1985, p. 104), the catchment relief ratio (Fryirs and Brierley, 2013, p. 35), and two variations of elongation ratio: (i) using a circle as a reference (Schumm, 1956), and (ii) using the catchment area as a reference (Fryirs and Brierley, 2013, p. 34).

6.3 Climatic indices

Numerous climatic attributes were estimated: annual mean of different variables (air temperature, potential evaporation, precipitation) over the entire studied period, aridity and seasonality indices, measure of the asynchronicity between the precipitation and potential evaporation, etc. The attributes that use potential evaporation are computed three times using Penman, Penman-Monteith and Oudin formulas. Attributes on heavy-precipitation days frequency (e.g. frequency of high-precipitation days, i.e. larger than 5 times the mean daily precipitation) and intensity (strongest rainfall on record), and dry-days frequency (average duration of dry periods, i.e. number of consecutive days with precipitation lower than 1 mm d^{-1}) were also computed. Time series of statistics at annual time step using hydrological year are also provided including annual daily maximum precipitation and annual seasonality index. As mentioned in Sect. 5.3, the first year (1970) is always missing. Furthermore, maps with resolution of $1 \times 1 \text{ km}^2$ of hourly and daily rainfall intensity, developed by Arnaud et al. (2008) from the SHYREG-Pluie database (Base de données SHYREG-Pluie © INRAE, 2016, all rights reserved), were used to calculate a normalized indicator of rainfall intensity at the catchment scale. This indicator is defined as the ratio of the hourly to daily rainfall intensity with 10-year return period (Poncelet, 2016).

6.4 Hydrometry

Several CAMELS-FR dataset attributes are related to streamflow data quality estimated for each gauging station. Some of these attributes are provided by the data producers. For example, the overall level of uncertainty is qualified by the producer for three flow ranges (high, mean and low flow). Moreover, several quality codes are associated to each streamflow value, depending on the way the value was estimated (classical flow estimation using a water level measurement and a rating curve, or a value reconstituted a posteriori) (see Sect. 5.2).

Note that this information lacks consistency throughout the CAMELS-FR catchment set, since this qualification is done by regional services, which have different qualification methods according to the regional hydroclimatic context.

Additional attributes were estimated for each station to describe the number of gaps over the studied period (e.g. percentage of missing data in the total period (1 January 1970 to 31 December 2021) and the overall percentage of streamflow data flagged

as questionable or as unqualified by the data producer. A simple algorithm was also applied to identify potential errors due to
315 linear interpolation between two values.

Finally, we attributed to each station an overall estimation of low-flow quality ~~was made~~ based on the visual analysis of temporal streamflow series: stations with low flows showing suspicious data or behaviour have been identified, in the CAMELS-FR dataset v1 showing 52 % of catchments with such issues.

6.5 Hydrological signatures

320 As for catchment climate, various hydrological attributes were estimated to describe the main catchment hydrological features. These include catchment aridity (i.e. the ratio of mean daily potential evaporation to mean daily precipitation), catchment yield, streamflow elasticity to precipitation, catchment seasonality (e.g. month with the minimum mean monthly streamflow). The baseflow index (BFI) was estimated following three different approaches: (i) method proposed by Ladson et al. (2013) that uses a digital filter, (ii) method proposed by Gustard and Tallaksen (2008) through linear interpolation of a five-day non-overlapping
325 streamflow minima (computed with the lfstad R-package; Laaha and Koffler, 2022), and (iii) method proposed by Pelletier and Andréassian (2020) that uses a conceptual quadratic reservoir model (computed with the baseflow R-package; Pelletier et al., 2021). For the latter, before calculating the BFI, we filled the gaps in time-series with GR6J-CemaNeige (Pushpalatha et al., 2011; Valéry et al., 2014a, b), using Penman (Penman, 1948), Penman-Monteith (Monteith, 1965), and Oudin (Oudin et al., 2005) formulas. However, we provide the BFI using only the Oudin potential evaporation formula because there were no
330 significant BFI differences when using other formulas. The other attributes that use potential evaporation are computed three times using the three selected formulas. Time series of statistics at annual time step are also provided for annual maximum daily streamflow and the mean monthly annual minimum streamflow (QMNA) using hydrological and calendar year respectively.

6.6 Hydrogeology

The average catchment permeability and porosity were estimated thanks to the GLobal HYdrogeology MaPS database (GL-
335 HYMPS v2.0) (Huscroft et al., 2018). The national hydrogeological reference map (BDLISA v3) (Brugeron et al., 2018; BRGM, 2022) was used to calculate the karstic portion of the catchments and the percentages of each catchment covered by different hydrogeological formations (e.g. bedrock, sedimentary, alluvial zones).

6.7 Geology

The Global Lithological Map database (GLiM v1.0) (Hartmann and Moosdorf, 2012) was used to characterize the catchment
340 geology. This database, available at the 0.5° spatial resolution, provided estimates of (i) the dominant geological class of each catchment and (ii) the percentages of different lithologies (e.g. metamorphics, carbonate sedimentary rocks, etc.; see Fig. 2c).

6.8 Soil

Soil characteristics were described using four datasets. First, the Global 1-km Gridded Thickness of Soil, Regolith, and Sedimentary Deposit Layers v1 produced by Pelletier et al. (2016) was cropped in order to estimate, for each catchment, (i) the mean soil depth and (ii) the distribution (percentiles) of the soil depths over the catchment. The European Soil Database Derived data (ESDD) (JRC et al., 2013a, b) provides soil attributes with resolution of $1 \times 1 \text{ km}^2$ for a topsoil layer and a subsoil layer with the boundary at 30 cm soil depth for clay, sand, silt and organic carbon content, bulk density, coarse fragments and total available water content (TAWC). We therefore, aggregated these two layers from ESDD using weighted arithmetic mean in cells based on their soil depth for each pixel. We consider the attribute "depth available to roots" as the correspondent soil depth for each pixel. For the aggregation of TAWC, instead of calculating the weighted arithmetic mean, we calculated the sum of the two layers. Then we cropped the raster for each catchment to extract the percentiles, mean and skeweness of each attribute for the topsoil and the aggregated layer. The EU-SoilHydroGrids v1.0 (Tóth et al., 2017) with resolution of $250 \times 250 \text{ m}^2$ was used to extract the saturated hydraulic conductivity. This dataset has seven soil layers at at 0, 5, 15, 30, 60, 100, and 200 cm depth. The first four layers, that are less than or equal to 30 cm depth, are considered as topsoil. Therefore, we aggregated these layers to provide information on topsoil (using the first four layers) and the total seven layers as well using depth-weighted harmonic mean. The hydraulic saturated conductivity was divided by 24 in order to provide the results in cm/hour, and then was cropped for each catchment to extract the percentiles, mean and skeweness. Finally, the TAWC was also estimated by INRAE over France from the Réservoir utile des sols de la France métropolitaine v1.2 database (Roman Dobarco et al., 2021; Le Bas, 2021) with resolution of $90 \times 90 \text{ m}^2$, providing another distribution of TAWC at the catchment scale.

6.9 Land cover

The CORINE Land Cover dataset was used to estimate, for each catchment, (i) the dominant land cover class and the (ii) percentage of each class, at two dates (French Ministry of the Environment, 1990, 2018). This analysis has been performed for all aggregation levels (1, 2 and 3) of the CORINE Land Cover classification.

6.10 Intervention degree

Influence level attributes gather (i) information given by the data producer on the estimated anthropogenic impacts on the observed streamflow time series (4 attributes) and (ii) metrics we calculated to estimate the influence of dams present within each catchment (3 attributes). Thus, we listed, for each catchment, the number of dams and the total volume of artificial storage.

7 Dataset description and add-on products

7.1 Illustration of several attributes of the CAMELS-FR dataset

Figure 5b shows the distribution of four climatic characteristics (mean annual precipitation, mean annual potential evaporation, seasonality index and max annual precipitation) of the CAMELS-FR dataset catchment set, grouped by hydrological

region (see Fig. 5a). The northwestern catchments have lower annual precipitation than those in the south, the latter being characterized by high variability in annual precipitation and also in mean annual potential evaporation. Southern catchments show lower seasonality index values, due to Mediterranean climate characterized by winter maximum for precipitation and significant summer drought (de Lavenne and Andréassian, 2018). Figure 5c shows each CAMELS-FR dataset catchment in a Budyko-type nondimensional space (Andréassian and Perrin, 2012) and for each hydrological region, showing the diversity of hydroclimatic context. Several catchments are located over the water limit ($Q = P$), or under the energy limit ($Q = P - PET$) due to potential misestimation of precipitation, potential evaporation or streamflow, errors in catchment area estimation, or non-conservative catchment behavior.

Figure 6 presents maps and distributions of three climatic attributes (mean annual precipitation, mean annual potential evaporation and seasonality index: one can clearly identify the regions with higher than average mean precipitation (Fig. 6a): Brittany in the West, and all the mountain ranges, i.e. Vosges, Jura, Alps, Massif central and the Pyrenees. Note that the spatial distribution of extreme precipitations shows a clear structure along a northwest-southeast axis (Fig. 6b), while potential evaporation is structured along a north-south axis, with some variations induced by the mountain ranges (Fig. 6c). Streamflow-related indices (Fig. 6d, 6e, 6f) do not show clear large-scale patterns, because they reflect the complex interplay between the climatic factors and the pedo-lithologic factors (see Fig. 2b & 2c).

7.2 CAMELS-FR add-on products

Two side-products were developed around the CAMELS-FR dataset, to provide tools to visualize catchment-scale time series, and synthetic summaries, to give the user a good overview of the data.

- CAMELS-FR graphical fact sheets (Delaigue et al., 2024a): static plots summarizing hydro-climatic, topographical, hydrogeological, and land cover data (available in English and French) (see example Fig. 7);
- CAMELS-FR time series dynamic graphs (Delaigue et al., 2024d): HTML pages with dynamic plots of hydroclimatic time series (click and drag zooming, and "onmouseover" display of legends and values; available in English and French) (see example Fig. 8).

8 Conclusions and perspectives

The CAMELS-FR dataset v1 gathers data over 654 catchments located in France, including daily hydroclimatic time series over the 1970-2021 period and 255 attributes split in 10 classes (see Tab. 2). These catchments represent a significant diversity of hydroclimatic contexts (e.g. snow- or groundwater-dominated catchments, Mediterranean catchments, etc.). The catchment selection was based on four criteria: (i) streamflow data availability over the 1970-2021 period, (ii) limited artificial influences (quantified based on upstream dam storage only), (iii) consistency between catchment area provided by the data producer and estimated by the DTM analysis and (iv) visual analysis of the streamflow time series (at the daily time step). We did not consider any selection criteria based on hydrological model efficiency.

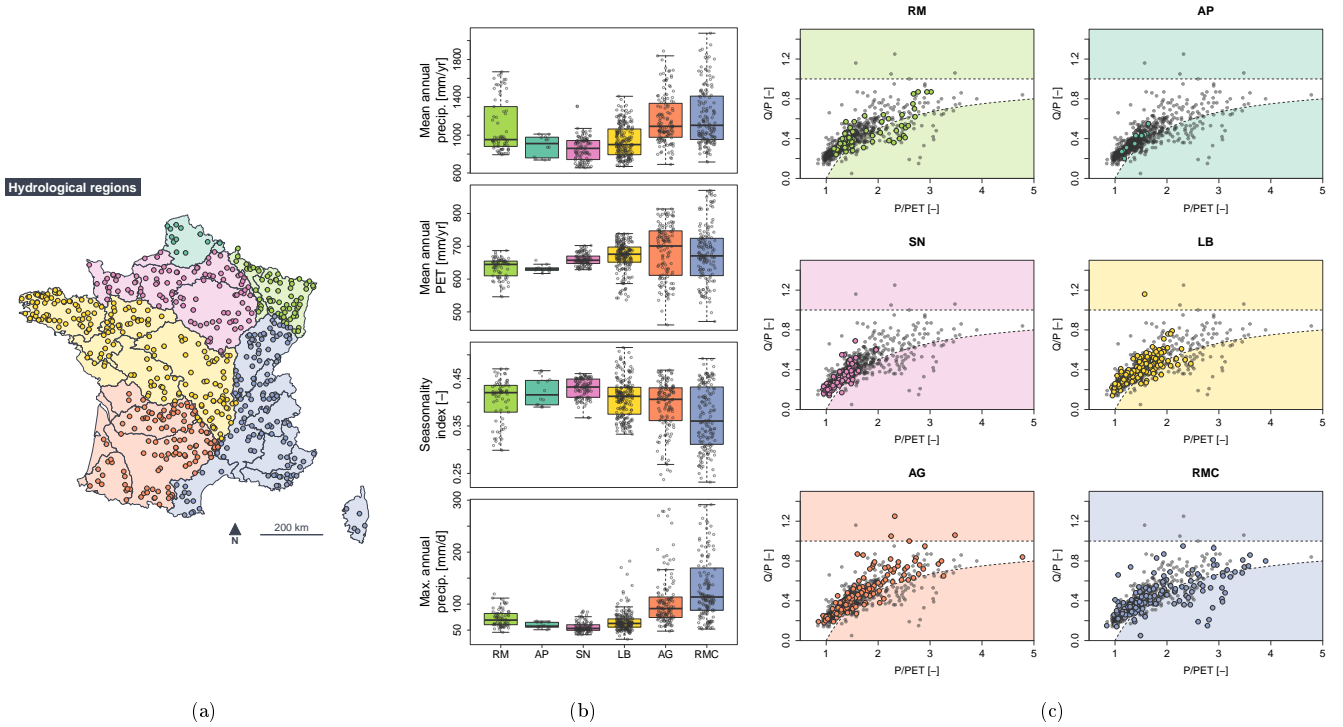


Figure 5. Distribution of CAMELS-FR catchment set over hydrological regions : (a) Geographical locations; (b) Boxplots of climatic indices; (c) Projection on a Budyko space (AG: Adour-Garonne, AP: Artois-Picardie, LB: Loire-Bretagne, RM: Rhin-Meuse, RMC: Rhône-Méditerranée-Corse, SN: Seine-Normandie; hydrological region boundaries: French water agencies, 2017a): (a) Geographical locations; (b) Boxplots of climatic indices; (c) Projection onto a Budyko-like space (large colored dots: catchments inside the given hydrological region; small grey dots: all the other catchments).

The CAMELS-FR dataset has been designed to be a "living" dataset. Several changes and updates are planned in subsequent versions: time series lengthening, streamflow values correction by the data producers, addition of "new" catchments (e.g. from French overseas territories). Versions with data at finer temporal and spatial resolutions may also be developed. A web-app devoted to the selection of catchment subsets using hydro-climatic, topographical, hydrogeological, or land cover criteria is currently under development. A CAMELS-FR dataset extension into the world-wide Caravan initiative (Kratzert et al., 2023) is also foreseen.

9 Code availability

The code sources are detailed in the description file available in the data repository (see below).

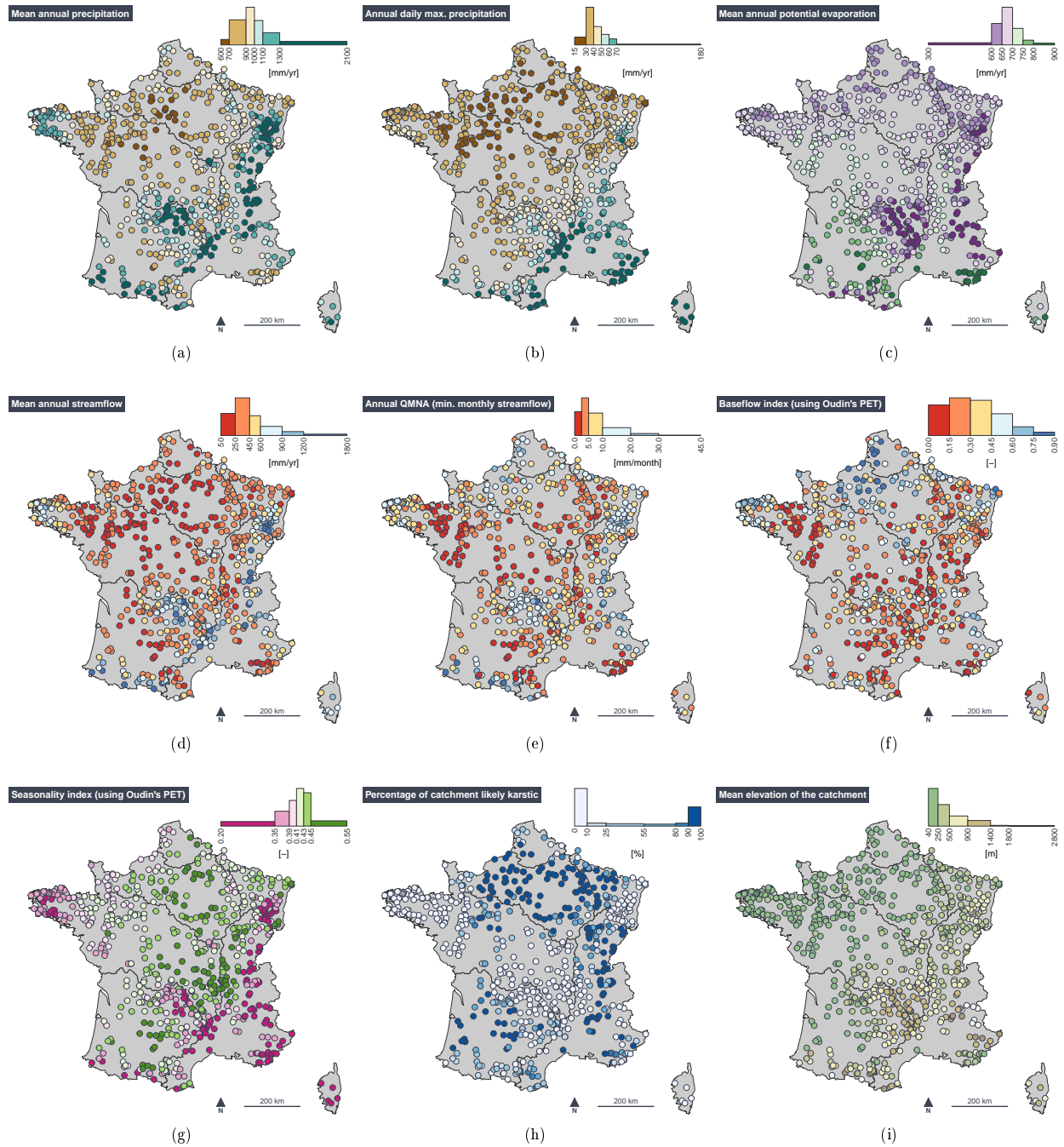


Figure 6. Maps and distributions of few catchment-scale attributes (hydrological region boundaries: French water agencies, 2017a). (a) Mean annual precipitation; (b) Mean annual daily maximum precipitation ; (c) Mean annual long-term potential evaporation (Oudin method); (d) Mean annual streamflow; (e) Mean annual minimum monthly streamflow (QMNA); (f) Baseflow index using (Pelletier and Andréassian, 2020); (g) Seasonality index (de Lavenne and Andréassian, 2018); (h) Percentage of catchment that is likely karstic; (i) Mean elevation of the catchment. Note that for those indices requiring a potential evaporation estimate, we used consistently the Oudin method.



Type	Source	Period	Time step
Streamflow	Hydroportal	1970-2021	Daily
Climate	SAFRAN (Météo-France)	1970-2021	Daily
DEM 100 m	SRTM (NASA)	2011	-
Extraction date	Hydroportal	2022-11-30	-
Interannual mean			
Streamflow	700 (50.7)		mm/yr (m ³ /s)
Precipitation (total / solid)	1044 / 495.7		mm/yr (m ³ /s)
PET (Penman-Monteith / Oudin)	537 / 405		mm/yr (m ³ /s)
Temperature	2.9		°C
Streamflow missing data			
Extreme values of the series			
Q ₄ max	17.4 (460.0)		mm/d (m ³ /s)
P ₂ max	88.3		mm/d
Q ₄ min	14.9		mm/month

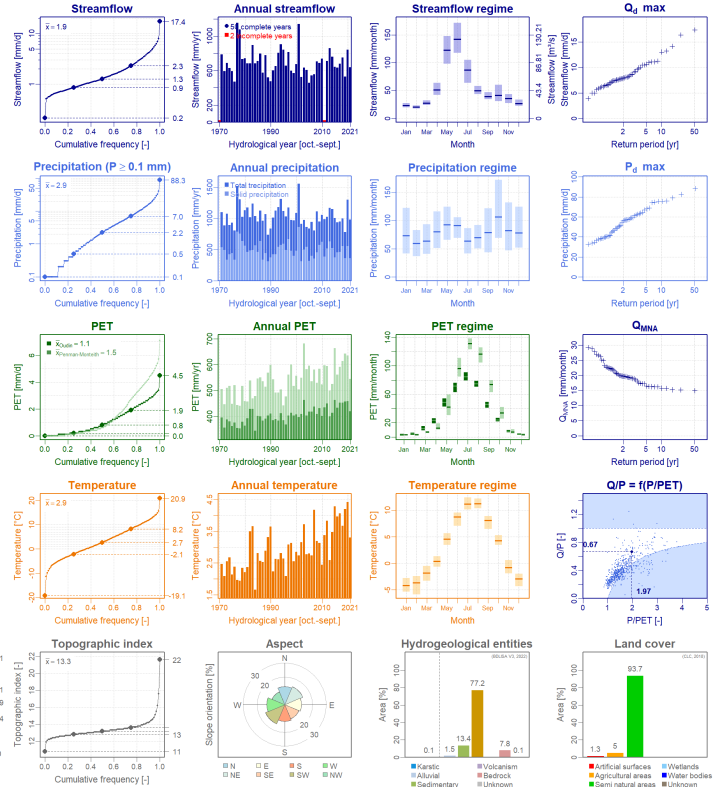
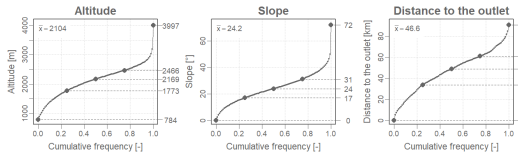
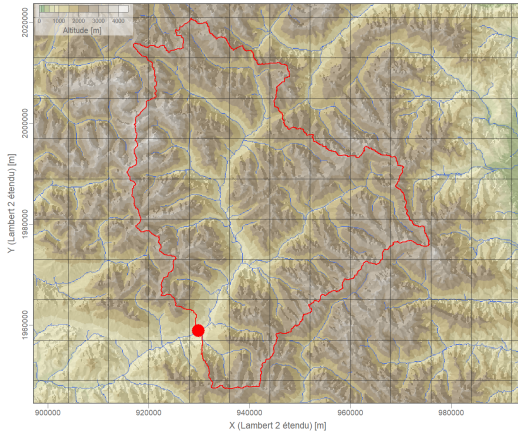


Figure 7. Example of CAMELS-FR graphical fact sheets (Delaigue et al., 2024a) for the X031001001 station ("La Durance à Embrun [La Clapière] - DREAL PACA").

10 Data availability

The CAMELS-FR dataset (Delaigue et al., 2024c) can be freely downloaded from the French governmental research data warehouse entrepot.recherche.data.gouv.fr using the following doi: [10.57745/WH7FJR](https://doi.org/10.57745/WH7FJR). The CAMELS-FR time series dynamic graphs (Delaigue et al., 2024d) and the CAMELS-FR graphical fact sheets (Delaigue et al., 2024a) also have their own digital object identifier, respectively doi: [10.57745/KK2SVJ](https://doi.org/10.57745/KK2SVJ) and doi: [10.57745/HBQWP5](https://doi.org/10.57745/HBQWP5).

Most of the variables included in the dataset are based on the French State Open License version 2.0 (<https://www.etalab.gouv.fr/licence-ouverte-open-licence>, last access: 23 October 2024), which is compatible with the CC BY license. A few are based either on CC BY licenses version 3 or 4, or on specific licenses (provided with the dataset). The CAMELS-FR dataset is distributed under the CC BY license version 4.0. (<https://creativecommons.org/licenses/by/4.0>, last access: 23 October 2024).

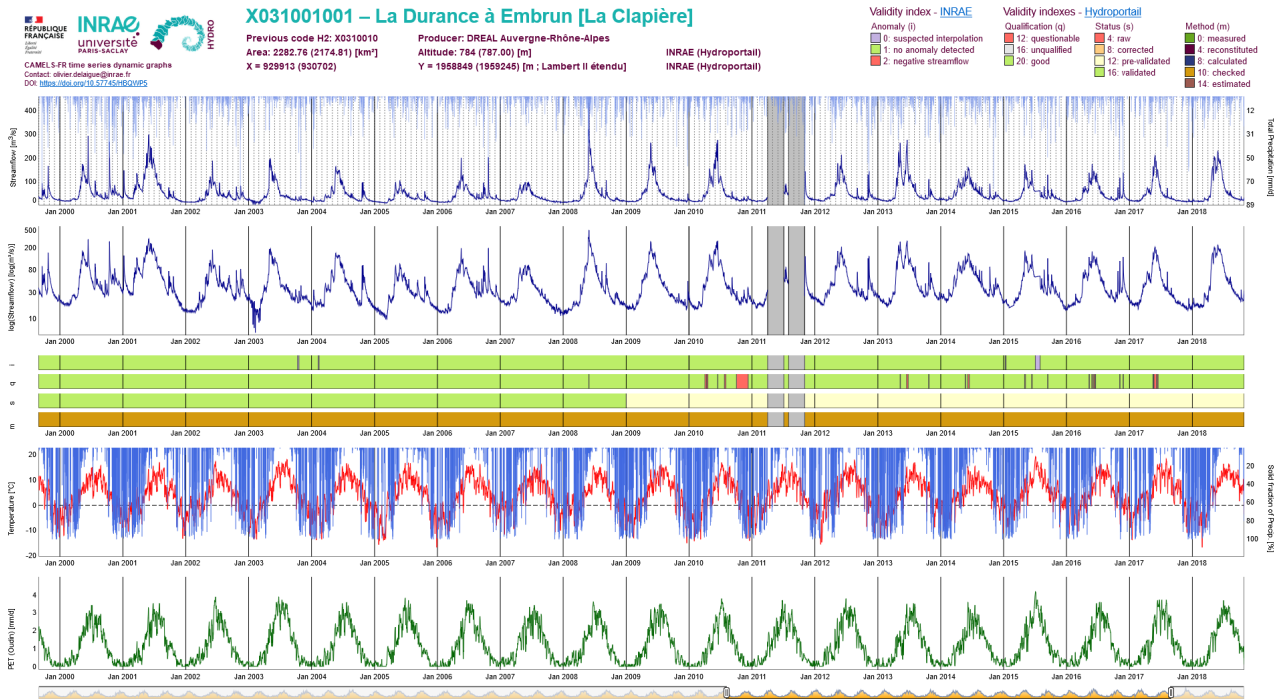


Figure 8. Example of CAMELS-FR time series dynamic graphs (Delaigue et al., 2024d) for the X031001001 station ("La Durance à Embrun [La Clapière] - DREAL PACA").

Each modification to the dataset can be tracked, as the version number will be automatically updated. Older releases will remain available, even if the data has been updated. A "NEWS" file will be updated in order to track changes between versions.

Author contributions. OD conceptualized the work. OD, GG, BG, PB, VA, and NA wrote the computer codes to format the data and calculate the indicators. OD, GG, PB, and CP visually inspected the streamflow time series. OD, GG, and PB assessed the locations and volumes of French reservoirs. OD, GG, PB, CP, and VA drafted the manuscript. All authors reviewed and edited the manuscript.

Competing interests. The contact author has declared that none of the authors has any competing interests.

Acknowledgements. The authors would like to thank colleagues from SCHAPI and DRIEAT: Jean-Nicolas Audouy, Carine Chaléon, and Stéphanie Pitsch for their essential help on the Hydroportail data. We would like to thank hydrological data producers for responding to our numerous requests to check, edit, and if necessary, correct Hydroportail data. We would like to thank Météo-France: Pierre Etchevers for supporting this endeavour, François Besson and Jean-Marie Willemet for providing data. We would like to thank OFB: Karl Kreutzenberger

430 for providing the GEOBS data, and Pierre Steinbach for his expertise on this database and for taking into account our suggestions of
modifications. We would like to thank many current or former members of the HYCAR research unit at INRAE for their contributions
to this database: François Bourgin, Pierre-Yves Bourgin, Mathilde Chauveau, Louise Crochemore, Andrea Ficchi, Carina Furusho-Percot,
Nicolas Le Moine, Laure Lebecherel, Florent Lobligois, Pierre Malassenne, Pierre Nicolle, Julien Peschard, Carine Poncelet, Maria-Helena
Ramos, Gaëlle Tallec, Guillaume Thirel, and Julie Viatgé. We wish to thank Jean-Nicolas Audouy, François Bourgin, Stéphanie Pitsch, and
435 Guillaume Thirel for their comments on the draft version of this manuscript. Last, we thank the comments from the associate editor Sibylle
Hasler, the reviewers Markus Hrachowitz and Larisa Tarasova, and Jospeh Janssen, which helped improving the quality of the paper.

References

- Addor, N., Newman, A. J., Mizukami, N., and Clark, M. P.: The CAMELS data set: catchment attributes and meteorology for large-sample studies, *Hydrology and Earth System Sciences*, 21, 5293–5313, <https://doi.org/10.5194/hess-21-5293-2017>, 2017.
- 440 Almagro, A., Oliveira, P. T. S., Meira Neto, A. A., Roy, T., and Troch, P.: CABra: a novel large-sample dataset for Brazilian catchments, *Hydrology and Earth System Sciences*, 25, 3105–3135, <https://doi.org/10.5194/hess-25-3105-2021>, 2021.
- Alvarez-Garretón, C., Mendoza, P. A., Boisier, J. P., Addor, N., Galleguillos, M., Zambrano-Bigiarini, M., Lara, A., Puelma, C., Cortes, G., Garreaud, R., McPhee, J., and Ayala, A.: The CAMELS-CL dataset: catchment attributes and meteorology for large sample studies – Chile dataset, *Hydrology and Earth System Sciences*, 22, 5817–5846, <https://doi.org/10.5194/hess-22-5817-2018>, 2018.
- 445 Andréassian, V. and Perrin, C.: On the ambiguous interpretation of the Turc-Budyko nondimensional graph, *Water Resources Research*, 48, <https://doi.org/10.1029/2012WR012532>, 2012.
- Andréassian, V., Perrin, C., Berthet, L., Le Moine, N., Lerat, J., Loumagne, C., Oudin, L., Mathevet, T., Ramos, M.-H., and Valéry, A.: HESS Opinions "Crash tests for a standardized evaluation of hydrological models", *Hydrology and Earth System Sciences*, 13, 1757–1764, <https://doi.org/10.5194/hess-13-1757-2009>, 2009.
- 450 Andréassian, V., Perrin, C., Parent, E., and Bárdossy, A.: The Court of Miracles of Hydrology: can failure stories contribute to hydrological science?, *Hydrological Sciences Journal*, 55, 849–856, <https://doi.org/10.1080/02626667.2010.506050>, 2010.
- Arnaud, P., Lavabre, J., Sol, B., and Descouches, C.: Regionalization of an hourly rainfall generating model over metropolitan France for flood hazard estimation, *Hydrological Sciences Journal*, 53, 34–47, <https://doi.org/10.1623/hysj.53.1.34>, 2008.
- Arsenault, R., Bazile, R., Ouellet Dallaire, C., and Brissette, F.: CANOPEX: A Canadian hydrometeorological watershed database, *Hydro-*
- 455 *logical Processes*, 30, 2734–2736, <https://doi.org/10.1002/hyp.10880>, 2016.
- Beven, K. J. and Kirby, M. J.: A physically based, variable contributing area model of basin hydrology / Un modèle à base physique de zone d'appel variable de l'hydrologie du bassin versant, *Hydrological Sciences Bulletin*, 24, 43–69, <https://doi.org/10.1080/02626667909491834>, 1979.
- Bourgin, P.-Y., Lobligeois, F., Peschard, J., Andréassian, V., Le Moine, N., Coron, L., Perrin, C., Ramos, M.-H., and Khalifa, A.: Description
- 460 des caractéristiques morphologiques, climatiques et hydrologiques de 4436 bassins versants français. Guide d'utilisation de la base de données hydro-climatique, Technical report, IRSTEA, <https://hal.science/hal-02596718>, (last access: 12 September 2024), 2010.
- BRGM: BDLISA. Base de donnée des limites des systèmes aquifères, <https://bdlisa.eaufrance.fr/>, version 3.0, (last access: 12 November 2023). Bureau de recherches géologiques et minières (BRGM), 2022.
- Brugeron, A., Paroissien, J., and Tillier, L.: Référentiel hydrogéologique BDLISA version 2 : Principes de construction et évolutions. Rapport
- 465 final, Tech. Rep. BRGM/RP-67489-FR, Bureau de recherches géologiques et minières (BRGM), 2018.
- CFBR: CFBR website, <https://www.barrages-cfbr.eu/>, (last access: 15 January 2023). Comité français des barrages et réservoirs (CFBR), 2023.
- Chagas, V. B. P., Chaffe, P. L. B., Addor, N., Fan, F. M., Fleischmann, A. S., Paiva, R. C. D., and Siqueira, V. A.: CAMELS-BR: hydrometeorological time series and landscape attributes for 897 catchments in Brazil, *Earth System Science Data*, 12, 2075–2096, <https://doi.org/10.5194/essd-12-2075-2020>, 2020.
- 470 Coxon, G., Addor, N., Bloomfield, J. P., Freer, J., Fry, M., Hannaford, J., Howden, N. J. K., Lane, R., Lewis, M., Robinson, E. L., Wagener, T., and Woods, R.: CAMELS-GB: hydrometeorological time series and landscape attributes for 671 catchments in Great Britain, *Earth System Science Data*, 12, 2459–2483, <https://doi.org/10.5194/essd-12-2459-2020>, 2020.

- de Lavenne, A. and Andréassian, V.: Impact of climate seasonality on catchment yield: A parameterization for commonly-used water balance formulas, *Journal of Hydrology*, 558, 266–274, <https://doi.org/10.1016/j.jhydrol.2018.01.009>, 2018.
- de Marsily, G., Combes, P., and Goblet, P.: Comment on ‘Ground-water models cannot be validated’, by L.F. Konikow & J.D. Bredehoeft, *Advances in Water Resources*, 15, 367–369, [https://doi.org/10.1016/0309-1708\(92\)90003-K](https://doi.org/10.1016/0309-1708(92)90003-K), 1992.
- Delaigue, O.: hydroportail: Retrieve French Hydrological Data from Hydroportail, <https://gitlab.irstea.fr/HYCAR-Hydro/hydroportail>, R package version 0.1.0.9006, (last access: 12 November 2023), 2022.
- 480 Delaigue, O., Brigode, P., Lobligeois, F., Bourgin, P.-Y., and Guimarães, G. M.: CAMELS-FR graphical fact sheets, <https://doi.org/10.57745/KK2SVJ>, V1, 2024a.
- Delaigue, O., Guimarães, G. M., Brigode, P., Andréassian, V., Payan, J.-L., Steinbach, P., and Kreutzenberger, K.: MADAM: Metropolitan Area Dams, <https://doi.org/10.57745/N98NEN>, V1, 2024b.
- Delaigue, O., Guimarães, G. M., Brigode, P., Génot, B., Perrin, C., and Andréassian, V.: CAMELS-FR dataset, 485 <https://doi.org/10.57745/WH7FJR>, V1, 2024c.
- Delaigue, O., Génot, B., and Guimarães, G. M.: CAMELS-FR time series dynamic graphs, <https://doi.org/10.57745/HBQWP5>, V1, 2024d.
- do Nascimento, T. V. M., Rudlang, J., Höge, M., van der Ent, R., Chappon, M., Seibert, J., Hrachowitz, M., and Fenicia, F.: ES-treams: An Integrated Dataset and Catalogue of Streamflow, Hydro-Climatic Variables and Landscape Descriptors for Europe, <https://doi.org/10.5281/zenodo.13961394>, 2024a.
- 490 do Nascimento, T. V. M., Rudlang, J., Höge, M., van der Ent, R., Chappon, M., Seibert, J., Hrachowitz, M., and Fenicia, F.: ES-treams: An integrated dataset and catalogue of streamflow, hydro-climatic and landscape variables for Europe, *Scientific Data*, 11, 879, <https://doi.org/10.1038/s41597-024-03706-1>, 2024b.
- Ducharne, A.: Reducing scale dependence in TOPMODEL using a dimensionless topographic index, *Hydrology and Earth System Sciences*, 13, 2399–2412, <https://doi.org/10.5194/hess-13-2399-2009>, 2009.
- 495 Farr, T. G., Rosen, P. A., Caro, E., Crippen, R., Duren, R., Hensley, S., Kobrick, M., Paller, M., Rodriguez, E., Roth, L., Seal, D., Shaffer, S., Shimada, J., Umland, J., Werner, M., Oskin, M., Burbank, D., and Alsdorf, D.: The Shuttle Radar Topography Mission, *Reviews of Geophysics*, 45, <https://doi.org/10.1029/2005RG000183>, 2007.
- Fitzpatrick, F. A.: Watershed Geomorphological Characteristics, in: *Handbook of applied hydrology*, edited by Singh, V. P., pp. 44–144–12, McGraw-Hill Education, New York, 2 edn., ISBN 978-0-07-183510-7, 2017.
- 500 Fowler, K. J. A., Acharya, S. C., Addor, N., Chou, C., and Peel, M. C.: CAMELS-AUS: hydrometeorological time series and landscape attributes for 222 catchments in Australia, *Earth System Science Data*, 13, 3847–3867, <https://doi.org/10.5194/essd-13-3847-2021>, 2021.
- French Ministry of the Environment: CORINE Land Cover. Occupation des sols en France, <https://www.data.gouv.fr/fr/datasets/corine-land-cover-occupation-des-sols-en-france/>, version 1990, (last access: 12 November 2023), 1990.
- French Ministry of the Environment: CORINE Land Cover. Occupation des sols en France, <https://www.data.gouv.fr/fr/datasets/corine-land-cover-occupation-des-sols-en-france/>, version 2018, (last access: 12 November 2023), 2018.
- 505 French water agencies: BD Carthage: Régions hydrographiques de Métropole 2017, <https://www.sandre.eaufrance.fr/atlas/srv/fre/catalog.search#/metadata/485cfb8d-602b-43bb-8d30-818beb31dc2b>, version 2021-06-09, (last access: 12 November 2023), 2017a.
- French water agencies: BD Carthage: Cours d’eau de Métropole 2017, <https://www.sandre.eaufrance.fr/atlas/srv/fre/catalog.search#/metadata/7381de46-42f7-42df-9abe-0ecd4b946034>, version 2019-10-24, (last access: 12 November 2023), 2017b.
- 510 Fryirs, K. A. and Brierley, G. J.: *Geomorphic analysis of river systems: an approach to reading the landscape*, Wiley-Blackwell, Chichester, 1 edn., ISBN 978-1-4051-9274-3, 978-1-4051-9275-0, 2013.

- Giuntoli, I., Renard, B., Vidal, J.-P., and Bard, A.: Low flows in France and their relationship to large-scale climate indices, *Journal of Hydrology*, 482, 105–118, <https://doi.org/10.1016/j.jhydrol.2012.12.038>, 2013.
- Gupta, H. V., Perrin, C., Blöschl, G., Montanari, A., Kumar, R., Clark, M., and Andréassian, V.: Large-sample hydrology: a need to balance
515 depth with breadth, *Hydrology and Earth System Sciences*, 18, 463–477, <https://doi.org/10.5194/hess-18-463-2014>, 2014.
- Gustard, A. and Tallaksen, L. M.: Low-Flow indices, in: *Manual on Low-flow Estimation and Prediction*, edited by Gustard, A. and Demuth, S., vol. 50 of *Operational hydrology report*, p. 138, WMO, Geneva, ISBN 978-92-63-11029-9, <https://library.wmo.int/records/item/32176-manual-on-low-flow-estimation-and-prediction>, 2008.
- Génot, B. and Delaigue, O.: Graphical user interface to help snapping hydrometric stations on the theoretical river network, INRAE, 2018.
- 520 Hartmann, J. and Moosdorf, N.: Global Lithological Map Database v1.0 (gridded to 0.5° spatial resolution), <https://doi.org/10.1594/PANGAEA.788537>, publication Title: Supplement to: Hartmann, Jens; Moosdorf, Nils (2012): The new global lithological map database GLiM: A representation of rock properties at the Earth surface. *Geochemistry, Geophysics, Geosystems*, 13, Q12004, <https://doi.org/10.1029/2012GC004370>, 2012.
- Hauße, C., Brandes, C., Lei, K., Pahner, S., Körner, P., Kronenberg, R., and Schuetze, N.: CAMELS-SAX: A meteorological and hydrological
525 dataset for spatially distributed modeling of catchments in Saxony, <https://doi.org/10.5194/egusphere-egu23-14357>, conference Name: EGU23, 2023.
- Hodgkins, G. A., Renard, B., Whitfield, P. H., Laaha, G., Stahl, K., Hannaford, J., Burn, D. H., Westra, S., Fleig, A. K., Araújo Lopes, W. T., Murphy, C., Mediero, L., and Hanel, M.: Climate Driven Trends in Historical Extreme Low Streamflows on Four Continents, *Water Resources Research*, 60, e2022WR034326, <https://doi.org/10.1029/2022WR034326>, e2022WR034326 2022WR034326, 2024.
- 530 Horton, R. E.: Drainage-basin characteristics, *Eos, Transactions American Geophysical Union*, 13, 350–361, <https://doi.org/10.1029/TR013i001p00350>, 1932.
- Huscroft, J., Gleeson, T., Hartmann, J., and Börker, J.: Compiling and mapping global permeability of the unconsolidated and consolidated Earth: GLobal HYdrogeology MaPS (GLHYMPS), <https://doi.org/10.5683/SP2/TTJNIU>, version 2.0, 2018.
- Höge, M., Kauzlaric, M., Siber, R., Schönenberger, U., Horton, P., Schwanbeck, J., Floriancic, M. G., Viviroli, D., Wilhelm, S.,
535 Sikorska-Senoner, A. E., Addor, N., Brunner, M., Pool, S., Zappa, M., and Fenicia, F.: CAMELS-CH: hydro-meteorological time series and landscape attributes for 331 catchments in hydrologic Switzerland, *Earth System Science Data Discussions*, pp. 1–46, <https://doi.org/10.5194/essd-2023-127>, 2023.
- IGN: BD ALTI, <https://geoservices.ign.fr/bdalti/>, version 1.0., (last access: 12 November 2023). Institut national de l’information géographique et forestière (IGN), 2001.
- 540 IGN: Plan IGN, <https://geoservices.ign.fr/planign>, version 2.0, (last access: 12 November 2023). Institut national de l’information géographique et forestière (IGN), 2020.
- INRAE: Base de données SHYREG-pluie, <https://shyreg.pluie.recover.inrae.fr/>, (last access: 8 November 2016). Institut national de recherche pour l’agriculture, l’alimentation et l’environnement (INRAE), 2016.
- JRC, IES, and Hiederer, R.: Mapping soil properties for Europe – Spatial representation of soil database attributes, Tech. rep., Joint Research
545 Centre and Institute for Environment and Sustainability, <https://doi.org/doi/10.2788/94128>, 2013a.
- JRC, IES, and Hiederer, R.: Mapping soil typologies – Spatial decision support applied to the European Soil Database, Tech. rep., Joint Research Centre and Institute for Environment and Sustainability, <https://doi.org/doi/10.2788/87286>, 2013b.
- Klingler, C., Schulz, K., and Herrnegger, M.: LamaH-CE: LARge-SaMPle DATA for Hydrology and Environmental Sciences for Central Europe, *Earth System Science Data*, 13, 4529–4565, <https://doi.org/10.5194/essd-13-4529-2021>, 2021.

- 550 Koch, J.: Catchment Dataset Denmark, <https://doi.org/10.22008/FK2/YCQXTR>, version 1.0, 2021.
- Kratzert, F., Nearing, G., Addor, N., Erickson, T., Gauch, M., Gilon, O., Gudmundsson, L., Hassidim, A., Klotz, D., Nevo, S., Shalev, G., and Matias, Y.: Caravan - A global community dataset for large-sample hydrology, *Scientific Data*, 10, 61, <https://doi.org/10.1038/s41597-023-01975-w>, 2023.
- Laaha, G. and Koffler, D.: Ifstat: Calculation of Low Flow Statistics for Daily Stream Flow Data,
555 <https://doi.org/10.32614/CRAN.package.Ifstat>, R package version 0.9.12, 2022.
- Ladson, A. R., Brown, R., Neal, B., and Nathan, R.: A Standard Approach to Baseflow Separation Using The Lyne and Hollick Filter, *Australasian Journal of Water Resources*, 17, 25–34, <https://doi.org/10.7158/13241583.2013.11465417>, 2013.
- Le Bas, C.: Carte de la Réserve Utile en eau issue de la Base de Données Géographique des Sols de France, <https://doi.org/10.15454/JPB9RB>, version 2.3, 2021.
- 560 Le Moigne, P., Besson, F., Martin, E., Boé, J., Boone, A., Decharme, B., Etchevers, P., Faroux, S., Habets, F., Lafaysse, M., Leroux, D., and Rousset-Regimbeau, F.: The latest improvements with SURFEX v8.0 of the Safran–Isba–Modcou hydrometeorological model for France, *Geoscientific Model Development*, 13, 3925–3946, <https://doi.org/10.5194/gmd-13-3925-2020>, 2020.
- Lehner, B. and Grill, G.: Global river hydrography and network routing: baseline data and new approaches to study the world’s large river systems, *Hydrological Processes*, 27, 2171–2186, <https://doi.org/10.1002/hyp.9740>, 2013.
- 565 Lehner, B., Verdin, K., and Jarvis, A.: New Global Hydrography Derived From Spaceborne Elevation Data, *Eos, Transactions American Geophysical Union*, 89, 93–94, <https://doi.org/10.1029/2008EO100001>, 2008.
- Linsley, R.: Rainfall-runoff models : an overview, in: Rainfall-runoff relationship, edited by Singh, V. P., pp. 3–22, Water Resources Publications, Chelsea, Michigan, U.S, bookcrafters inc. edn., ISBN 978-0-918334-45-9, meeting Name: International Symposium on Rainfall Runoff Modeling, 1982.
- 570 Liu, J., Koch, J., Stisen, S., Troldborg, L., Højberg, A. L., Thodsen, H., Hansen, M. F. T., and Schneider, R. J. M.: CAMELS-DK: Hydrometeorological Time Series and Landscape Attributes for 3330 Catchments in Denmark, *Earth System Science Data Discussions*, 2024, 1–30, <https://doi.org/10.5194/essd-2024-292>, 2024.
- Loritz, R., Dolich, A., Acuña Espinoza, E., Ebeling, P., Guse, B., Götte, J., Hassler, S. K., Hauße, C., Heidbüchel, I., Kiesel, J., Mälicke, M., Müller-Thomy, H., Stölzle, M., and Tarasova, L.: CAMELS-DE: hydro-meteorological time series and attributes for 1555 catchments in
575 Germany, *Earth System Science Data Discussions*, 2024, 1–30, <https://doi.org/10.5194/essd-2024-318>, 2024.
- Miller, V. C. A.: Quantitative Geomorphic Study of Drainage Basin Characteristics in the Clinch Mountain Area, Virginia and Tennessee, Tech. Rep. 3, Columbia University, Department of Geology, New York, 1953.
- Monteith, J.: Evaporation and environment, *Symposia of the Society for Experimental Biology*, 19, 205–234, <http://europepmc.org/abstract/MED/5321565>, 1965.
- 580 Newman, A. J., Clark, M. P., Sampson, K., Wood, A., Hay, L. E., Bock, A., Viger, R. J., Blodgett, D., Brekke, L., Arnold, J. R., Hopson, T., and Duan, Q.: Development of a large-sample watershed-scale hydrometeorological data set for the contiguous USA: data set characteristics and assessment of regional variability in hydrologic model performance, *Hydrology and Earth System Sciences*, 19, 209–223, <https://doi.org/10.5194/hess-19-209-2015>, 2015.
- NOAA: Global Self-consistent, Hierarchical, High-resolution Geography Database (GSHHG), <https://www.ngdc.noaa.gov/mgg/shorelines/>,
585 version 2.3.7, (last access: 12 November 2023). National Oceanic and Atmospheric Administration (NOAA), 2017.

- OFB and partners: Géoréférenceur des obstacles [Application GEOBS, en ligne], Référentiel des obstacles à l'écoulement (Module 1, ROE) et Base de données complémentaire sur les obstacles à l'écoulement (Module 3, BDOe), <https://geobs.eaufrance.fr/>, version 2023-02-21, (last access: 12 November 2023). Office français de la biodiversité (OFB), 2023.
- Oudin, L., Hervieu, F., Michel, C., Perrin, C., Andréassian, V., Anctil, F., and Loumagne, C.: Which potential evapotranspiration input for a lumped rainfall–runoff model?: Part 2-Towards a simple and efficient potential evapotranspiration model for rainfall–runoff modelling, *Journal of Hydrology*, 303, 290–306, <https://doi.org/10.1016/j.jhydrol.2004.08.026>, 00236, 2005.
- Payan, J.-L.: Prise en compte de barrages-réservoirs dans un modèle global pluie-débit, Ph.D. thesis, ENGREF (AgroParisTech), <http://theses.hal.science/pastel-00003555>, 2007.
- Payan, J.-L., Perrin, C., Andréassian, V., and Michel, C.: How can man-made water reservoirs be accounted for in a lumped rainfall-runoff model?, *Water Resources Research*, 44, W03 420, <https://doi.org/10.1029/2007WR005971>, 2008.
- Peel, M. C., Finlayson, B. L., and McMahon, T. A.: Updated world map of the Köppen-Geiger climate classification, *Hydrology and Earth System Sciences*, 11, 1633–1644, <https://doi.org/10.5194/hess-11-1633-2007>, 2007.
- Pelletier, A.: Nappes et rivières : la piézométrie peut-elle améliorer la prévision des étiages des cours d'eau ?, Ph.D. thesis, Sorbonne Université, Paris, France, <https://theses.hal.science/tel-03783485>, 2021.
- Pelletier, A. and Andréassian, V.: Hydrograph separation: an impartial parametrisation for an imperfect method, *Hydrology and Earth System Sciences*, 24, 1171–1187, <https://doi.org/10.5194/hess-24-1171-2020>, 2020.
- Pelletier, A., Andréassian, V., and Delaigue, O.: baseflow: Computes Hydrograph Separation, <https://doi.org/10.15454/Z9IK5N>, R package version 0.13.2, 2021.
- Pelletier, J. D., Broxton, P. D., Hazenberg, P., Zeng, X., Troch, P. A., Niu, G., Williams, Z. C., Brunke, M. A., and Gochis, D.: Global 1-km Gridded Thickness of Soil, Regolith, and Sedimentary Deposit Layers, ORNL DAAC, <https://doi.org/10.3334/ORNLDAAAC/1304>, 2016.
- Penman, H. L.: Natural evaporation from open water, bare soil and grass, *Proceedings of the Royal Society of London. Series A. Mathematical and Physical Sciences*, 193, 120–145, <https://doi.org/10.1098/rspa.1948.0037>, 1948.
- Perrin, C., Michel, C., and Andréassian, V.: Improvement of a parsimonious model for streamflow simulation, *Journal of Hydrology*, 279, 275–289, [https://doi.org/10.1016/S0022-1694\(03\)00225-7](https://doi.org/10.1016/S0022-1694(03)00225-7), 2003.
- Poncelet, C.: Du bassin au paramètre : jusqu'où peut-on régionaliser un modèle hydrologique conceptuel ?, Ph.D. thesis, Université Pierre et Marie Curie - Paris VI, Antony, France, <https://theses.hal.science/tel-01529196>, 2016.
- Pushpalatha, R., Perrin, C., Le Moine, N., Mathevet, T., and Andréassian, V.: A downward structural sensitivity analysis of hydrological models to improve low-flow simulation, *Journal of Hydrology*, 411, 66–76, <https://doi.org/10.1016/j.jhydrol.2011.09.034>, 2011.
- Quintana-Segui, P., Le Moigne, P., Durand, Y., Martin, E., Habets, F., Baillon, M., Canellas, C., Franchisteguy, L., and Morel, S.: Analysis of near-surface atmospheric variables: Validation of the SAFRAN analysis over France, *Journal of Applied Meteorology and Climatology*, 47, 92–107, <https://doi.org/10.1175/2007JAMC1636.1>, 2008.
- Rabus, B., Eineder, M., Roth, A., and Bamler, R.: The shuttle radar topography mission—a new class of digital elevation models acquired by spaceborne radar, *ISPRS Journal of Photogrammetry and Remote Sensing*, 57, 241–262, [https://doi.org/10.1016/S0924-2716\(02\)00124-7](https://doi.org/10.1016/S0924-2716(02)00124-7), 2003.
- Refsgaard, J. C. and Hansen, J. R.: A good-looking catchment can turn into a modeller's nightmare, *Hydrological Sciences Journal*, 55, 899–912, <https://doi.org/10.1080/02626667.2010.505571>, 2010.
- Roman Dobarco, M., Bourennane, H., Arrouays, D., Saby, N., Cousin, I., and Martin, M. P.: Réservoir utile des sols de la France métropolitaine, <https://doi.org/10.15454/9IRARJ>, version 1.2, 2021.

- Schaake, J., Cong, S., and Duan, Q.: The US mopex data set, IAHS Publication Series, 307, 9–28, <https://www.osti.gov/biblio/899413>, 2006.
- 625 Schumm, S. A.: Evolution of Drainage Systems & Slopes in Badlands at Perth, New Jersey, Geological Society of America Bulletin, 67, 597, [https://doi.org/10.1130/0016-7606\(1956\)67\[597:EODSAS\]2.0.CO;2](https://doi.org/10.1130/0016-7606(1956)67[597:EODSAS]2.0.CO;2), 1956.
- Strohmenger, L., Sauquet, E., Bernard, C., Bonneau, J., Branger, F., Bresson, A., Brigode, P., Buzier, R., Delaigue, O., Devers, A., Evin, G., Fournier, M., Hsu, S.-C., Lanini, S., de Lavenne, A., Lemaitre-Basset, T., Magand, C., Mendoza Guimarães, G., Mentha, M., Munier, S., Perrin, C., Podechard, T., Rouchy, L., Sadki, M., Soutif-Bellenger, M., Tilmant, F., Tramblay, Y., Véron, A.-L., Vidal, J.-P., and Thirel, G.:
- 630 On the visual detection of non-natural records in streamflow time series: challenges and impacts, Hydrology and Earth System Sciences, 27, 3375–3391, <https://doi.org/10.5194/hess-27-3375-2023>, 2023.
- Strohmenger, L., Collet, L., Andréassian, V., Corre, L., Rousset, F., and Thirel, G.: Köppen–Geiger climate classification across France based on an ensemble of high-resolution climate projections, Comptes Rendus. Géoscience, 356, 67–82, <https://doi.org/10.5802/crgeos.263>, 2024.
- 635 Subramanya, K.: Engineering Hydrology, McGraw Hill Education, New Delhi, 4 edn., ISBN 978-1-259-02997-4, 2013.
- Tramblay, Y., Rouché, N., Paturel, J.-E., Mahé, G., Boyer, J.-F., Amoussou, E., Bodian, A., Dacosta, H., Dakhlaoui, H., Dezetter, A., Hughes, D., Hanich, L., Peugeot, C., Tshimanga, R., and Lachassagne, P.: ADHI: the African Database of Hydrometric Indices (1950–2018), Earth System Science Data, 13, 1547–1560, <https://doi.org/10.5194/essd-13-1547-2021>, 2021.
- Tóth, B., Weynants, M., Pásztor, L., and Hengl, T.: 3D soil hydraulic database of Europe at 250 m resolution, Hydrological Processes, 31, 2662–2666, <https://doi.org/10.1002/hyp.11203>, 2017.
- 640 Valéry, A., Andréassian, V., and Perrin, C.: ‘As simple as possible but not simpler’: What is useful in a temperature-based snow-accounting routine? Part 1 – Comparison of six snow accounting routines on 380 catchments, Journal of Hydrology, 517, 1166–1175, <https://doi.org/10.1016/j.jhydrol.2014.04.059>, 2014a.
- Valéry, A., Andréassian, V., and Perrin, C.: ‘As simple as possible but not simpler’: What is useful in a temperature-based snow-accounting routine? Part 2 – Sensitivity analysis of the Cemaneige snow accounting routine on 380 catchments, Journal of Hydrology, 517, 1176–1187, <https://doi.org/10.1016/j.jhydrol.2014.04.058>, 2014b.
- 645 Vidal, J., Martin, E., Franchistéguy, L., Baillon, M., and Soubeyroux, J.: A 50-year high-resolution atmospheric reanalysis over France with the Safran system, International Journal of Climatology, 30, 1627–1644, <https://doi.org/10.1002/joc.2003>, 2010.
- Vincent, C., Peyaud, V., Laarman, O., Six, D., Gilbert, A., Gillet-Chaulet, F., Berthier, E., Morin, S., Verfaillie, D., Rabatel, A., Jourdain, B., and Bolibar, J.: Déclin des deux plus grands glaciers des Alpes françaises au cours du XXI^e siècle : Argentière et Mer de Glace, La
- 650 Météorologie, pp. 49–58, <https://doi.org/10.4267/2042/70369>, 2019.
- Wessel, P. and Smith, W. H. F.: A global, self-consistent, hierarchical, high-resolution shoreline database, Journal of Geophysical Research: Solid Earth, 101, 8741–8743, <https://doi.org/10.1029/96JB00104>, 1996.
- Zăvoianu, I.: Morfometria bazinelor hidrografice, Editura Academiei Republicii Socialiste România, Bucharest, 1978.
- 655 Zăvoianu, I.: Morphometry of drainage basins, no. 20 in Developments in water science, Elsevier, Amsterdam, Oxford, New York, Tokyo, 2 edn., ISBN 978-0-444-99587-2, 1985.